ORIGINAL ARTICLE
Cardiovascular Disorders

JKMS

http://dx.doi.org/10.3346/jkms.2015.30.5.576 • J Korean Med Sci 2015; 30: 576-585

The Effect of Umbilical Cord Blood Derived Mesenchymal Stem Cells in Monocrotaline-induced Pulmonary Artery Hypertension Rats

Hyeryon Lee,[1] Jae Chul Lee,[1] Jung Hyun Kwon,[1] Kwan Chang Kim,[2] Min-Sun Cho,[3] Yoon Sun Yang,[4] Wonil Oh,[4] Soo Jin Choi,[4] Eun-Seok Seo,[5] Sang-Joon Lee,[5] Tae Jun Wang,[6] and Young Mi Hong[1]

Departments of [1]Pediatrics, [2]Thoracic and Cardiovascular Surgery, and [3]Pathology, Ewha Womans University School of Medicine, Seoul; [4]Biomedical Research Institute, MEDIPOST, Co., Seoul; [5]Division of Integrative Bioscience and Bioengineering, [6]Division of Integrative Biosciences and Biotechnology, Pohang University of Science and Technology, Pohang, Korea

Received: 8 October 2014
Accepted: 16 January 2015

Address for Correspondence:
Young Mi Hong, MD
Department of Pediatrics, School of Medicine, Ewha Womans University, 1071 Anyangcheon-ro, Yangcheon-gu, Seoul 158-710, Korea
Tel: +82.2-2650-2841, Fax: +82.2-2653-3718
E-mail: ymhong@ewha.ac.kr

Funding: This research was supported by Basic Science Research Program through the National Research Foundation of Korea (NRF) funded by the Ministry of Education (2013R1A1A3004619).

Pulmonary arterial hypertension (PAH) causes right ventricular failure due to a gradual increase in pulmonary vascular resistance. The purposes of this study were to confirm the engraftment of human umbilical cord blood-mesenchymal stem cells (hUCB-MSCs) placed in the correct place in the lung and research on changes of hemodynamics, pulmonary pathology, immunomodulation and several gene expressions in monocrotaline (MCT)-induced PAH rat models after hUCB-MSCs transfusion. The rats were grouped as follows: the control (C) group; the M group (MCT 60 mg/kg); the U group (hUCB-MSCs transfusion). They received transfusions via the external jugular vein a week after MCT injection. The mean right ventricular pressure (RVP) was significantly reduced in the U group after the 2 week. The indicators of RV hypertrophy were significantly reduced in the U group at week 4. Reduced medial wall thickness in the pulmonary arteriole was noted in the U group at week 4. Reduced number of intra-acinar muscular pulmonary arteries was observed in the U group after 2 week. Protein expressions such as endothelin (ET)-1, endothelin receptor A (ERA), endothelial nitric oxide synthase (eNOS) and matrix metalloproteinase (MMP)-2 significantly decreased at week 4. The decreased levels of ERA, eNOS and MMP-2 immunoreactivity were noted by immnohistochemical staining. After hUCB-MSCs were administered, there were the improvement of RVH and mean RVP. Reductions in several protein expressions and immunomodulation were also detected. It is suggested that hUCB-MSCs may be a promising therapeutic option for PAH.

Keywords: Hypertension; Pulmonary; Monocrotaline; Cord Blood Stem Cell Transfusion; Gene Expression

INTRODUCTION

Pulmonary artery hypertension (PAH) leads to right ventricular failure and premature death (1). Although the pathophygiological mechanisms of PAH are not known exactly, the key element in the pathogenesis of PAH is known as intima and media proliferation and its consequent pulmonary vascular obstruction (2). PAH has been characterized as a disease of endothelial dysfunction with an imbalance between vasoconstrictors and vasodilators (3). With the identification of nitric oxide (NO) as an endothelium derived relaxing factor several studies have shown that PAH patients may have a reduced expression of eNOS in the vascular endothelium of the pulmonary arteries (4), although this has been contested by others (5).

There are several PAH animal models including chronic hypoxia (6), monocrotaline (MCT) injury (7) and hypoxia-Sugen 5416 (8). From among these models, the most commonly used models of PAH are the chronic hypoxia model and the MCT injury model (9). MCT is a pyrrolizidine alkaloid that causes a PAH in rats. Although the toxicological mechanisms of MCT are unclear, MCT pneumotoxicity is most widely used as a model of human pulmonary hypertension (7). It is difficult to make an early diagnosis and have a full recovery from PAH. There are difficulties in recovering pulmonary artery blood pressure using conventional drugs such as vasodilator, prostacyclin and anti-coagulants.

Human umbilical cord blood-mesenchymal stem cell (hUCB-MSC)s have recently been studied to evaluate their potential as a source of cell therapy (10). hUCB-MSCs could be a breakthrough to other incurable diseases because hUCB-MSCs can substitute impaired vascular cells by paracrine-mediated effects and direct trans-differentiations in stem cells (11). However, it is rare to study hUCB-MSCs in PAH.

The purposes of this study were to confirm the engraftment

pISSN 1011-8934
eISSN 1598-6357

of hUCB-MSCs in the lung and investigate changes of pulmonary pathology, hemodynamics, immunomodulation and several gene expressions in MCT-induced PAH rat models after hUCB-MSCs injection.

MATERIALS AND METHODS

Animals

We used six-week-old male Sprague-Dawley rats for this research. All rats were kept in climate-controlled conditions with a 12 hr light/12 hr dark cycle, and were given full access to food and water. Pulmonary hypertension was induced by subcutaneous (sc) injection of 60 mg/kg MCT (Sigma Chemicals, St. Louis, MO, USA) dissolved in 0.5 N HCl solution. The rats were grouped as follows: control (C) group (n = 16), sc injection of saline, M group (n = 24), sc injection of MCT; hUCB-MSCs transfusion (U group) (n = 24). hUCB-MSCs (3×10^6 cells/rat) were administered throught the external jugular vein 1 week after MCT injection. The animals were sacrificed at weeks 1, 2, and 3 after hUCB-MSCs transfusion. Tissues were extracted and were frozen right away at -70°C.

Estimation of mean RVP

The animals were put in the supine position and instrumented with an arterial pressure line (Physiological Pressure Transducer, MLT1199; AD Instruments, Oxfordshire, UK). Hemodynamic parameters were recorded at baseline and at weeks 2, 3, and 4. The catheter was put into the external jugular vein to estimate mean right ventricular pressure (RVP).

Organ weights

The rats were weighed and observed for general appearance throughout the research period. The animals were sacrificed at the scheduled time. The right ventricle (RV), left ventricle (LV) +septum (S), lung and kidney were weighed. We calculated organ/body weight × 1,000. The RV to LV+S ratio (RV/[LV+S]) was used as an index of right ventricular hypertrophy (RVH). This method is based on our previous reports (12, 13).

Two-photon microscopy

Two-photon microscopy (TPM) obtained 3-D images by acquiring x-y plane images sequentially, while moving its focal plane stepwise in the z axis. In this experiment, two-photon excitation wavelength we used was 750 nm for excitation of autofluorescence and 1,050 nm for excitation of PKH26. Laser power at lung tissue sample was 72 mW and 36 mW in the case of 750 nm and 1,050 nm, respectively. The excitation focus scanned in the x-y plane of the sample by the scanners, and in the z axis by an objective translator P-725.4CL (Physik Instrumente, Karlsruhe, Germany). Emission light from the sample was collected back by the objective lens and was reflected on dichroic mirror (DM, 680DCLP, Chroma, Rockingham, VT, USA) toward photomultiplier tubes (PMTs, R5929, Hamamatsu, Japans). We calculated PKH26 density % area using Image J software.

Histopathological examination

3 μm sections of paraffin thickness were stained with hematoxylin & eosin and Victoria blue straining. We used visual imaging system to disitize the image digitized by using image-Pro plus 6.0 program. Measurements were randomly made on 30 muscular arteries per lung section in 25-100 μm sized vessels in each photographic field. We measured the medial wall thickness between the internal and external elastic lamina of two sides of muscular arteries (M1 and M2). The percentage of wall thickness was calculated as follows: % wall thickness = (M1+M2)/diameter of the vessel × 100. For pathological assessment of neomuscularization, the numbers of the muscularized vessels with diameter < 50 μm were measured in a × 200 magnification field below the terminal bronchiole. Twenty fields were examined in each rat for this analysis (13).

Western blot analysis

The tissues were homogenized in 10 mM Tris HCl buffer, pH 7.4 containing 0.5 mM EDTA, pH 8.0, 0.25 M sucrose, 1 mM PMSF, 1 mM Na_4VO_3 and a protease inhibitor cocktail (Roche-Boehringer-Mannheim, Mannheim, Germany). After centrifugation, the supernatant was subjected to sodium dodecyl sulfate polyacrylamide gel electrophoresis (SDS-PAGE). Samples equivalent to 25 μg of protein content were loaded and size-separated in 8%-12% SDS-PAGE. The proteins on the acrylamide gel were transferred to a polyvinylidene difluoride membrane (Millipore, Bedford, MA, USA) at 400 mA in a transfer buffer containing 25 mM Tris and 192 mM glycine, pH 8.4. The nitrocellulose membranes was blocked in TBS with 5% non-fat dry milk at room temperature for 1 hr in 0.1% Tween 20 and incubated with the optimal primary antibodies, including ET-1 (SantaCruz biotechnology, Santacruz, CA, USA), ERA (SantaCruz biotechnology, Santacruz, CA, USA), eNOS (SantaCruz biotechnology, Santacruz, CA, USA), and MMP-2 (Cell Signaling Technology Inc., Danvers, MA, USA) and GAPDH (SantaCruz biotechnology, Inc., Santacruz, CA, USA), at 4°C overnight. The membrane was incubated with horseradish peroxidase-conjugated secondary antibody (Cell Signaling Technology Inc., Danvers, MA, USA) for 1 hr at room temperature. After washing, the membrane was visualized by a chemiluminescent reaction using an ECL-detection kit system from GE Healthcare (Amersham Bioscience, Piscataway, NJ, USA).

Cell preparation

hUCB-MSCs were obtained from Medipost Inc. (Biomedical research institute Co., Ltd, Seoul, Korea) and isolated human MSCs were expanded in culture according to the method of the

previous report (14). Briefly, mononuclear cells (MNCs) isolated from hUCB were washed, suspended in alpha-minimum essential medium (α-MEM, Gibco-Invitrogen, Carlsbad, CA, USA) supplemented with 10% fetal bovine serum (FBS, Gibco-Invitrogen, Grand island, NY, USA). hUCB-MSCs were attached to plastic culture dishes during the culture period and exhibited spindle-shaped fibroblast-like morphology at passage 5.

Immunohistochemistry

We incubated the lung tissues overnight in 10% buffered formalin. Four-micron sections were cut from paraffin embedded tissue blocks and deparaffinized in zylene and rehydrated in graded alcohols (100%-70%). Heat antigen retrieval was obtained by boiling of tissue sections in antigen retrieval solution pH 6.0 or pH 9.0 (Dako, Carpinteria, CA, USA) for 10 min in microwave prior to incubation at 4°C overnight with primary antibodies against ET-1 (SantaCruz biotechnology, Santacruz, CA, USA), ERA (SantaCruz biotechnology, Santacruz, CA, USA), eNOS (SantaCruz biotechnology, Santacruz, CA, USA) and MMP-2 (Abcam, Campridge, UK). After incubation with the optimal biotinylated secondary antibodies for 30 min at 4°C and afterwards with a streptavidin (Dako, Kyoto, Japan), color development was done using 3-amino-9-ethylcarbazole or DAB as a chromogen.

Cytokine array and gene expression in lung tissues

Lung samples were collected at termination (3 week after hUCB-MSCs injection) and quickly frozen in liquid nitrogen. A rat cytokine array (ARY008, R&D Systems, Minneapolis, MN, USA) was performed on lung homogenates according to manufacturer's instructions to screen whether hUCB-MSCs treatment suppress local secretion of specific inflammatory cytokines by

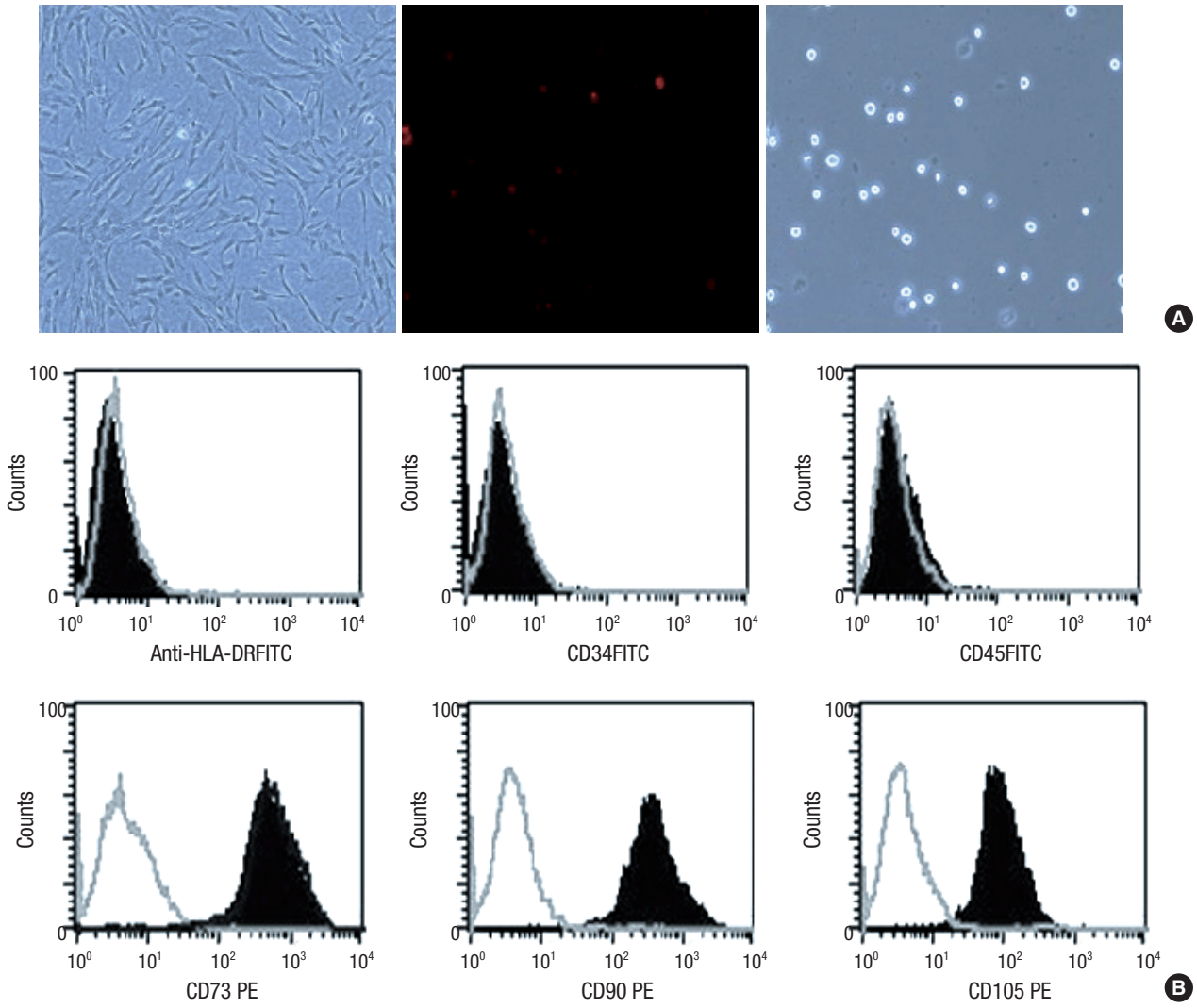

Fig. 1. Human UCB-MSCs preparation. Characterization of hUCB-MSCs at passage 5. hUCB-MSCs by phase-contrast microscopy (**A**). Cells grow uniformly and have a spindle-shape (left). PKH26-labeled MSCs are stained in red (middle, × 200). Immunophenotype from UCB-hMSCs (**B**). These cells are positive for antigens CD73, CD90 and CD105 but generally not for antigens HLA-DR, CD34 and CD45. The gray lines indicate the isotype matched mouse IgG antibody control labeling.

http://dx.doi.org/10.3346/jkms.2015.30.5.576

the host lung cells. Samples were pooled per treatment group and equal amounts of protein were loaded on the blots. From all pooled samples blots were performed in duplicate and averages of these two pixel densities were used to calculate the average density with Image J software. Background staining and spot size were analyzed as recommended by the manufacturer. Briefly, pictures were converted to 8-bit inverted jpeg files and spots were encircled. Per blot, equal spot sizes were analyzed.

Statistical analysis

Results are showed as the means ± standard deviation. We used an unpaired two-tailed *t*-test and Mann-Whitney test. We considered a P value < 0.05 statistically significant. SPSS 14.0 for Windows (SPSS, Chicago, IL, USA) was used for all statistical analyses.

Ethics statement

All animal experimental procedures were approved by the institutional animal care and use committee (IACUC) of the School of Medicine of Ewha Womans University in 2013 (approval number. 13-0234).

RESULTS

Characterization and immunophenotype from hUCB-MSCs

We found that hUCB-MSCs grew uniformly. They appeared to be spindle-shaped (left). PKH26-labeled hUCB-MSCs were stained in red (middle). We did not observe any trypan blue positive cells (red: PKH26, blue: trypan blue) (Fig. 1A). The cells were positive for the cell surface markers CD73, CD90, and CD105, but negative for the hematopoietic cell-specific surface markers CD34, CD45, as well as for the MHC class II marker HLA-DR. The gray lines indicate the isotype matched the mouse Ig G antibody control labeling (Fig. 1B). We were able to identify hUCB-MSCs at passage 5 with a CD73+, CD90+, CD105+, CD34-, CD45-, and HLA-DR. hUCB-MSCs did not express hematopoietic markers; CD45+, CD34+, CD105-, CD73-, CD90-. Characterization of hUCB-MSCs by flow cytometry was performed in a cultured cells.

Engraftment of hUCB-MSCs in the lung tissues

We confirmed that the hUCB-MSCs were engrafted in the lung tissues using two-photon microscopy. In the U group, white circular forms were observed at 1,050 nm wave length which could be hUCB-MSCs. These white circular forms in the U group were more lighter in color compared than those in both C and M group (Fig. 2). PKH-26 detection % area was greater in the U group than the C or M group (C vs. M vs. U; 1.00 vs. 0.87 vs. 1.43)

Changes in RVP and RV/LV+S after hUCB-MSCs injection in PAH rats

The mean RVP was significantly increased in the M group compared with the C group at weeks 2, 3, and 4. RVP was significantly decreased in the U group compared with the M group at weeks 2, 3, and 4 (Table 1). RV/LV+S was significantly increased in the M group at weeks 2, 3, and 4. RV/LV+S was significantly decreased in the U group at 4 week (Table 2).

Organ weight

The body weight was significantly decreased in the M group compared with the C group at weeks 3 and 4. The RV/body weight was significantly increased in the M group compared with the C group at weeks 2, 3, and 4 and significantly decreased in the

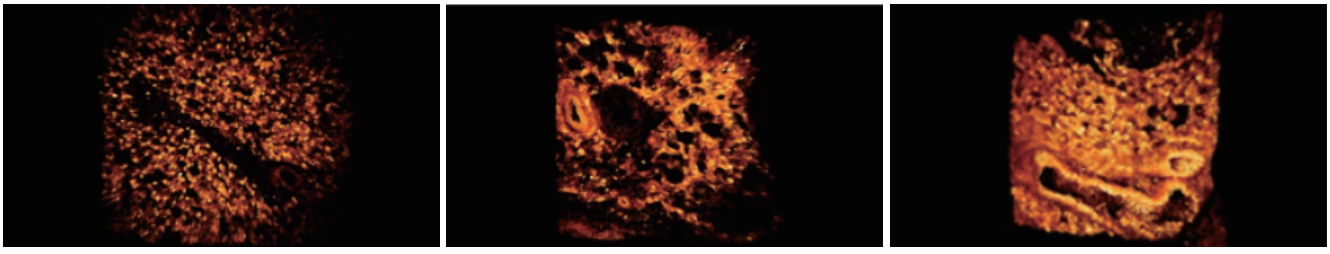

Fig. 2. Engraftment of hUCB-MSCs in lung tissues. The hUCB-MSCs tagged by PKh-26 are observed at 1,050 nm wave length in the lung tissues. Light circular forms are considered to UCB-MSCs engrafted. C, control group; M, monocrotaline group; U, hUCB-MSCs group (Field of view: 300 μm).

Table 1. Changes of right ventricular pressure after hUCB-MSCs injection in PAH rats (mmHg)

Week	C	M	U
2	11.0 ± 0.0	36.5 ± 3.1*	23.6 ± 7.6†
3	11.5 ± 0.7	37.2 ± 6.3*	21.3 ± 4.9†
4	10.5 ± 2.1	52.0 ± 19.7*	16.5 ± 3.6†

*P < 0.05 compared with the C group; †P < 0.05 compared with the M group. C, control group; M, monocrotaline group; U, hUCB-MSCs group. Values are means ± SD.

Table 2. Changes of RV/LV+S ratio after hUCB-MSCs injection in PAH rats

Week	C	M	U
2	1.00 ± 0.05	1.47 ± 0.18*	1.43 ± 0.14
3	1.00 ± 0.46	2.89 ± 0.43*	2.18 ± 0.45
4	1.00 ± 0.07	2.88 ± 0.58*	1.85 ± 0.28†

*P < 0.05 compared with the C group; †P < 0.05 compared with the M group. C, control group; M, monocrotaline group; U, hUCB-MSCs group. Values are means ± SD.

Table 3. Changes of body and organ weights after hUCB-MSCs injection in PAH rats

Week	Group	Body Wt (g)	RV/Body Wt	LV/Body Wt	Lung/Body Wt	Kidney/Body Wt	Liver/Body Wt
2	C	338.63 ± 13.88	0.62 ± 0.02	2.20 ± 0.05	4.18 ± 0.34	4.35 ± 0.16	4.21 ± 0.18
	M	278.50 ± 27.69	1.01 ± 0.10*	2.34 ± 0.11	7.10 ± 1.15*	4.33 ± 0.50	4.77 ± 0.29*
	U	308.56 ± 25.85	1.14 ± 0.21	2.43 ± 0.17	8.50 ± 1.37	4.52 ± 0.36	4.31 ± 0.41
3	C	293.75 ± 19.45	0.40 ± 0.18	1.99 ± 0.00	3.24 ± 0.14	4.01 ± 0.14	4.14 ± 0.31
	M	266.67 ± 54.35*	1.62 ± .0.24*	2.16 ± 0.08	10.05 ± 3.67*	4.15 ± 0.32	4.07 ± 0.31
	U	251.00 ± 37.94	1.72 ± 0.33	2.32 ± 0.23	10.93 ± 2.10	4.37 ± 0.40	4.22 ± 0.40
4	C	404.00 ± 36.77	0.61 ± 0.04	0.61 ± 0.04	3.68 ± 0.05	4.26 ± 0.30	3.77 ± 0.30
	M	248.89 ± 40.96*	2.67 ± 0.04*	2.67 ± 0.04	9.28 ± 3.29*	4.38 ± 0.38	3.90 ± 0.49
	U	279.29 ± 26.58	1.81 ± 0.15†	1.81 ± 0.15	8.92 ± 1.67	4.02 ± 0.21	3.69 ± 0.39

*$P < 0.05$ compared with the C group; †$P < 0.05$ compared with the M group. C, control; M, monocrotaline; U, hUCB-MSCs; Wt, weight; RV, right ventricle; LV, left ventricle. Values are means ± SD.

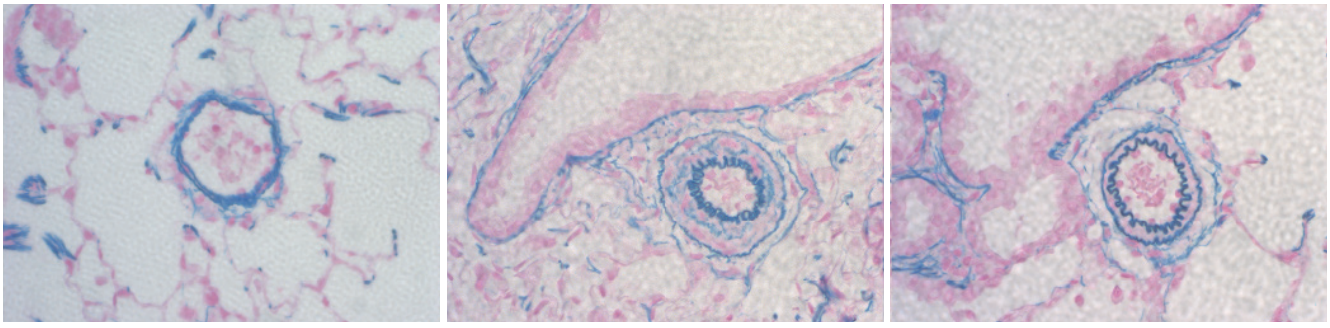

Fig. 3. Photographs of peripheral pulmonary arteries in the three groups after Victoria blue straining (×400). The medial layer of the pulmonary arterioles thickened progressively after the monocrotaline injection. The medial wall thicknesses was significantly reduced in the U group at week 4. C, control; M, monocrotaline; U, hUCB-MSCs.

U group compared to the M group at week 4. The lung/body weight was significantly increased in the M group compared with the C group at weeks 2, 3, and 4 (Table 3).

Pathological changes in the lung tissues

Fully muscularized arteries were only seen in pulmonary arterioles (> 10 μM, < 100 μM) in the M group and the U group. Pulmonary arterioles in the U group showed decreased tendency of medial wall thickening by Victoria blue straining (Fig. 3).

The M group showed a significant increase in medial wall thickness compared to the C group at weeks 2, 3, and 4. The U group showed significant reductions in medial thickness at the 4 week compared with the M group (Table 4A, Fig. 3).

The number of muscular intra-acinar arteries in the M group was significantly increased compared to the C group at weeks 2, 3, and 4 and significantly decreased in the U group at weeks 2, 3, and 4 compared with the M group (Table 4B, Fig. 3).

Immunohistochemistry analysis in the lung tissues

Immunohistochemical expressions revealed that the positive cells of ET-1, ERA, eNOS, and MMP-2 were significantly higher in the M group than the C group, however, ERA, eNOS, and MMP-2 were lower in the U group than the M group (Fig. 4A). This result indicated that hUCB-MSCs could attenuate the vascular remodeling. The increased levels of ET-1, ERA, eNOS, and MMP-2 immunoreactivity observed in the M group were statistically significant. Three weeks after hUCB-MSCs transfusion, levels of ERA, eNOS, and MMP-2 immunoreactivity were significantly decreased in the U group compared with the M group (Fig. 4B).

Table 4. Changes of medial wall thickness and the number of intra acinar-arteries after hUCB-MSCs injection in PAH rats

A. Medial wall thickness

Week	C	M	U
1	25.9 ± 0.4	25.3 ± 2.2	28.4 ± 3.3
2	22.1 ± 2.9	38.5 ± 4.0*	34.2 ± 4.0
3	23.7 ± 1.0	38.8 ± 6.3*	33.2 ± 3.9
4	22.5 ± 0.4	32.3 ± 2.5*	37.3 ± 1.5†

B. The number of intra-acinar arteries

Week	C	M	U
1	1.16 ± 0.18	1.62 ± 0.20	1.79 ± 0.02
2	0.71 ± 0.07	2.01 ± 0.11*	1.61 ± 0.20†
3	1.05 ± 0.04	2.23 ± 0.29*	1.27 ± 0.02†
4	1.15 ± 0.22	2.78 ± 0.40*	1.45 ± 0.34†

*$P < 0.05$ compared with the C group; †$P < 0.05$ compared with the M group. C, control group; M, monocrotaline group; U, hUCB-MSCs group. Values are means ± SD.

Western blot analysis in the lung tissues

The protein expressions of ET-1, ERA, eNOS, and MMP-2 were significantly increased in the M group compared with the C

http://dx.doi.org/10.3346/jkms.2015.30.5.576

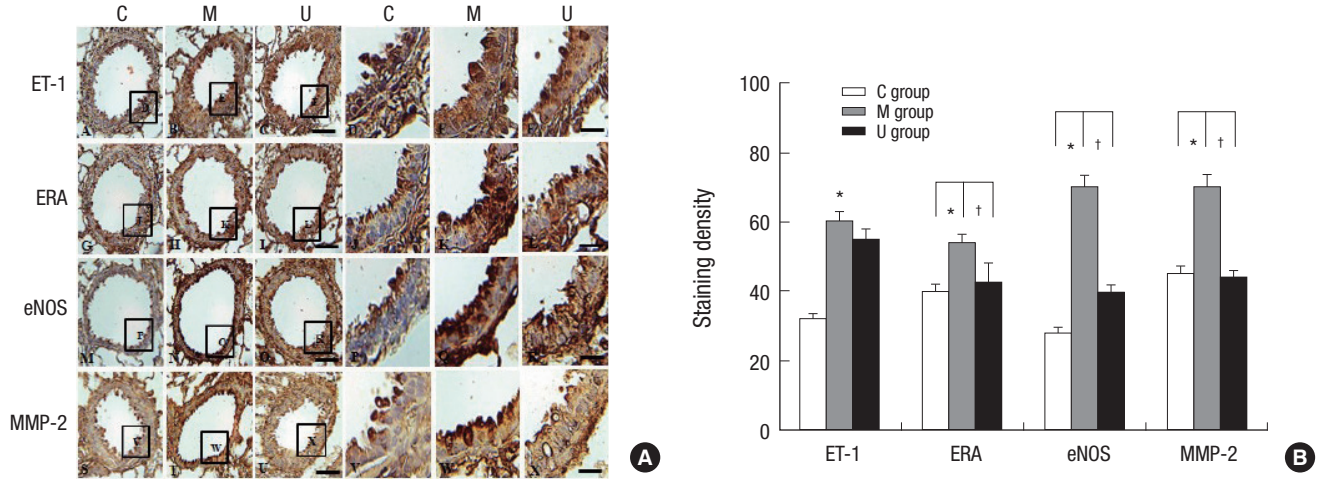

Fig. 4. Localization of ET-1, ERA, eNOS and MMP2-immunoreactive cells in the lung tissues at week 4. Immunohistochemical expressions revealed that the positive cells of ET-1, ERA, eNOS, and MMP-2 were significantly higher in the M group than the C group, however, they were lower in the U group than the M group (**A**). The increased levels of ET-1, ERA, eNOS, and MMP-2 immunoreactivity observed in the M group were statistically significant. The levels of ERA, eNOS, and MMP-2 immunoreactivity were significantly decreased in the U group compared with the M group (**B**). *$P < 0.05$ compared with the C group. †$P < 0.05$ compared with the M group. C, control group; M, monocrotaline group; U, hUCB-MSCs group. Scale bars = 40 μm (A-C, G-I, M-O, S-U), 10 μm (D-F, J-L, P-R, V-X).

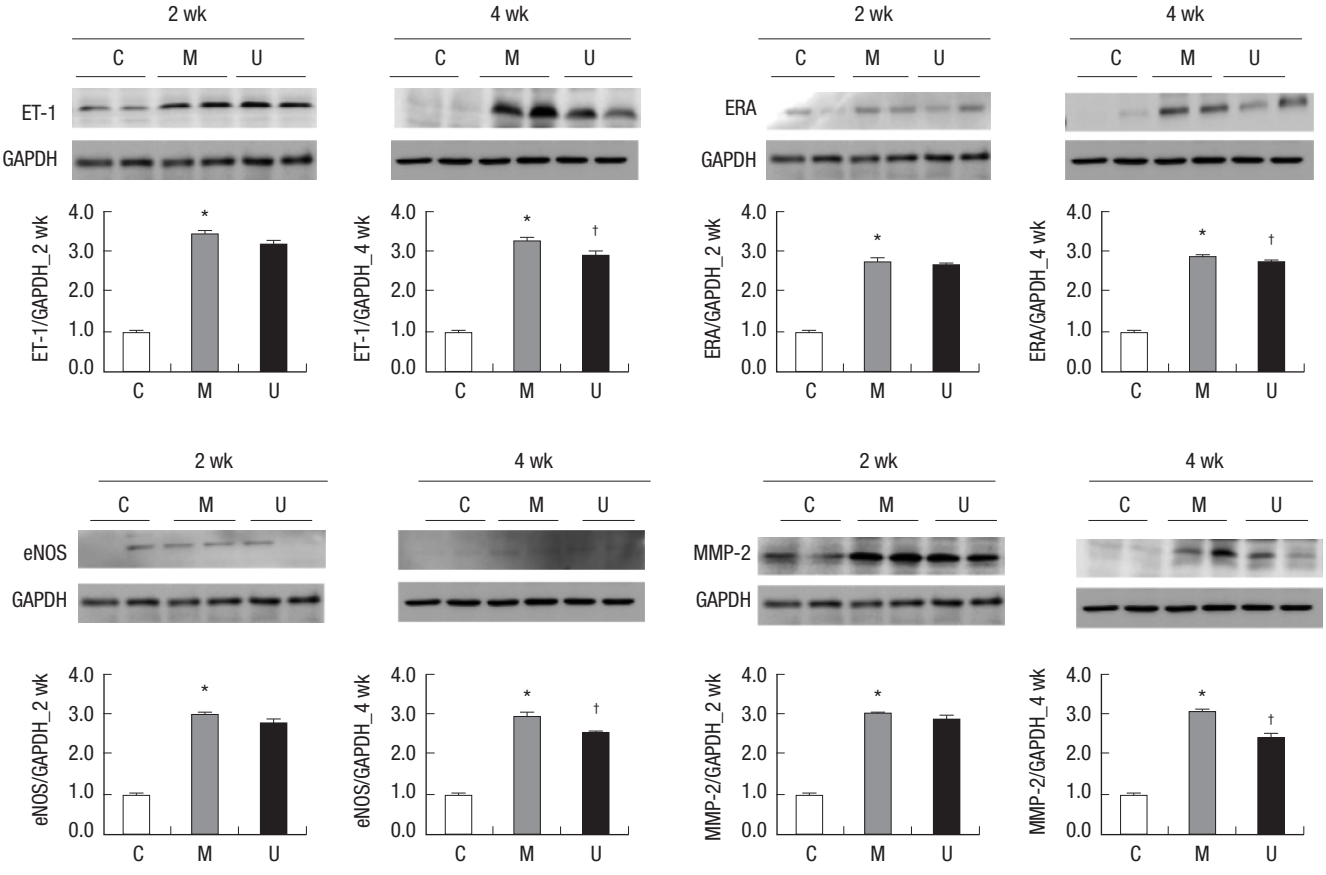

Fig. 5. Changes of ET-1, ERA, eNOS, and MMP-2 protein expression levels after hUCB-MSCs injection in PAH rats. These are pictures of protein expression levels of ET-1, ERA, eNOS, and MMP-2 in the lung tissues. The protein expression levels of ET-1, ERA, eNOS, and MMP-2 were significantly increased in the M group compared with the C group at weeks 2 and 4. The protein expression levels of ET-1, ERA, eNOS and MMP-2 were significantly decreased at week 4. *$P < 0.05$ compared with the C group, †$P < 0.05$ compared with the M group. C, control group; M, monocrotaline group; U, hUCB-MSCs group.

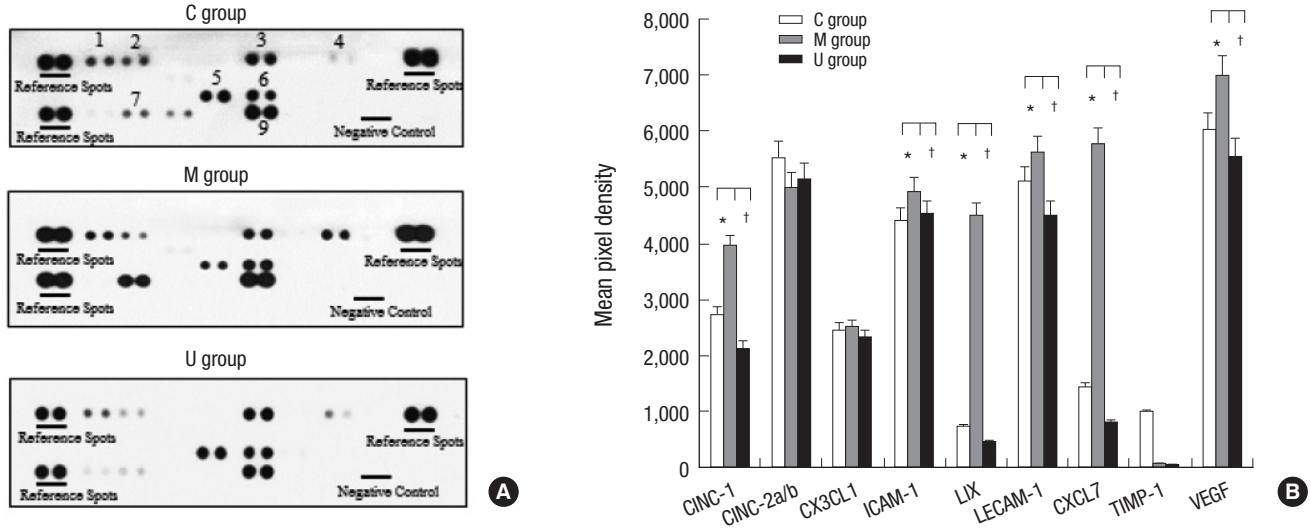

Fig. 6. Inflammatory cytokine expressions in the lung tissues. To screen whether hUCB-MSCs affected local production of inflammatory cytokines by lung cells in three groups, a cytokine array was performed on lung homogenates (**A**) CINC-1, ICAM-1, LIX, LECAM-1, CXCL7, and VEGF were higher in the M group, whereas CINC-1, ICAM-1, LIX, LECAM-1, CXCL7, and VEGF were lower in the U group compared to the M group. CINC-2a/b, CX3CL1, and TIMP-1 were not different in three groups (**B**). White bars, control (n = 6); gray bars, monocrotaline (n = 6); black bars, hUCB-MSCs (n = 7). CINC-1, cytokine-induced neutrophil chemoattractant-1; CINC-2a/b, cytokine-induced neutrophil chemoattractant-2a/b; CX3CL1, chemokine (C-X-C motif) ligand 1; ICAM, inter-cellular adhesion molecule; LIX, lipopolysaccharide-induced CXC chemokine; LECAM-1, leukocyte endothelial cell adhesion molecule 1; CXCL7, chemokine (C-X-C motif) ligand 7; TIMP-1, tissue inhibitor of metalloproteinase 1; VEGF, vascular endothelial growth factor. $^{*}P < 0.05$ compared with the C group, $^{\dagger}P < 0.05$ compared with the M group. C, control; M, monocrotaline; U, hUCB-MSCs.

group at weeks 2 and 4. The protein expressions of ET-1, ERA, eNOS, and MMP-2 were significantly decreased in the U group compared with the M group at week 4 (Fig. 5).

Cytokine profile is altered after hUCB-MSCs treatment in the lung tissues

To screen whether hUCB-MSCs affected local production of inflammatory cytokines to many kinds of cells in the lung tissues in three groups, a cytokine array was performed on lung homogenates (Fig. 6A). Nine inflammatory cytokines such as cytokine-induced neutrophil chemoattractant-1 (CINC-1); cytokine-induced neutrophil chemoattractant-2a/b (CINC-2a/b); chemokine (C-X-C motif) ligand 1 (CX3CL1); inter-cellular adhesion molecule 1 (ICAM-1); lipopolysaccharide-induced CXC chemokine (LIX); leukocyte endothelial cell adhesion molecule 1 (LECAM-1); chemokine (C-X-C motif) ligand 7 (CXCL7); tissue inhibitor of metalloproteinase 1 (TIMP-1) and vascular endothelial growth factor (VE-GF) were performed in three groups. CINC-1, ICAM-1, LIX, LECAM-1, CXCL7, and VEGF were higher in the M group, whereas CINC-1, ICAM-1, LIX, LECAM-1, CXCL7, and VEGF were lower in the U group compared to the M group. CINC-2a/b, CX3CL1, and TIMP-1 were not different in three groups (Fig. 6B).

DISCUSSION

In this study, we demonstrated that hUCB-MSCs (3×10^6 cells/rat) which were injected via the external jugular vein in the lung tissues of MCT-induced PAH rats. It remained for 3 weeks after injection. Adverse effects were not observed after hUCB-MSCs transfusion. hUCB-MSCs attenuated MCT-induced PAH. The mean RVP was significantly reduced in the U group after 2 week. The RV/LV+S ratio and RV/body weight were significantly decreased at week 4; Decreased number of intra-acinar muscular arteries was noted after 2 week and significant reductions in medial thickness of pulmonary arterioles were also observed at the 4 week; Protein expressions such as ET-1, ERA, eNOS, and MMP-2 significantly decreased at week 4; The decreased levels of ERA, eNOS, and MMP-2 immunoreactivity were observed by immnohistochemical staining at week 4.

We confirmed by two photon microscopy that hUCB-MSCs were engrafted in the lung tissues. PKH-26 labled hUCB-MSCs were identified for 3 weeks after injection in the lung tissues. They were clustered in a circular form and weakly spread in the extracellular matrix of lung tissues in PAH rats. This means that hUCB-MSCs injected via the external jugular vein can be widely distributed in the lung tissues by pulmonary arterioles and remain for at least 3 weeks. Also, we noted that the injected cells were engrafted more in the damaged area of the lung. In this study, MCT may cause a rapid progression of PAH before hUCB-MSCs produce effect including paracrine effect such as anti-inflammatory cytokine effect. As already known, most stem cells need transdifferentiation. It takes time to show therapeutic effect of hUCB-MSCs because MCT already caused histomorphologic changes in the lungs and RV.

Vascular remodeling occurred in our PAH rats. Vascular re-

http://dx.doi.org/10.3346/jkms.2015.30.5.576

modeling is accompanied by a thickening of the arterieal wall after 2 week which is thought to increase resistance by physical encroachment of the lumen of small peripheral pulmonary arteries and arterioles. Angiogenesis in pulmonary vessels also occurred in the MCT treated groups. The number of intraacinar arteries were increased in the M group after 2 week. The protein expressions of ET-1, ERA, eNOS, and MMP-2 were significantly increased in the M group after 2 week.

Immunohistochemical staining revealed that the positive cells of ET-1, ERA, eNOS, and MMP-2 expression were significantly higher in endothelium and smooth muscle layers in the M group.

We suggested the effects of hUCB-MSCs on ET-1, ERA, eNOS, and MMP-2. First, a key regulator of PAH, ET-1 was increased in the M group. Under the influence of hUCB-MSCs, the protein expression level of ET-1 was decreased in the U group. Second, ERA was increased in the M group. The protein expression level of ERA was significantly decreased in the U group. Presently, there are several types of ET receptor antagonists including bosentan, ambresentan and sataxentan (15). But these non-peptide chemical drugs have little effect on PAH in contrast with hUCB-MSCs. Third, NO, synthesized largely by eNOS in endothelial cell (EC), is a vasodilator and a suppressor of smooth muscle cell (SMC) proliferation. ECs in PAH patients, produce decreased amounts of NO. In our study, the eNOS expression level was increased in the M group and UCB-MSCs had a significantly decreased effect on eNOS. Although the molecular mechanisms of pulmonary vascular remodeling is unclear, certain extracellular matrix (ECM) components are likely to be involved. PAH is characterized by an accumulation of ECM component in the lung including MMP-2. It is known to be involved in the migration and proliferation in SMCs, and ECs. There have already been reports that MMP-2 expression is increased in PAH. Our data also shows similar results compared with our previous data (12).

hUCB-MSCs are regarded as an alternative source of bone marrow-derived MSCs because the collection of cord blood is less invasive than that of bone marrow. The clinical use of bone marrow MSCs has presented problems, including pain, morbidity, and age-related diseases (16). Our present study revealed that the effect of hUCB-MSCs seems to be superior to bone marrow cells in the depression of gene expressions when we compared with our previous studies (13).

The mechanisms underlying the possible in vivo immunomodulatory effects of hUCB-MSCs remain a critical and unresolved question (17). Cytokines and chemokines are known to play important roles in a number of biological processes, including immunity, apoptosis, angiogenesis and cell differentiation (18). Many of these processes are involved in pathogenesis and therapy (18). LIX, CXCL7 and CINC-1 are member of the CXC chemokine family which are potent neutrophil chemoattractants. ICAM-1 and LECAM-1 have been reported to inhibit the interaction between T cells and block NK cell-mediated toxicity, suggesting a pathogenesis promoting role (19). Recently, the role of VEGF have also been suggested in PAH (20). VEGF may be an important mediator of lung growth and responsible for angiogenesis and vasculogenesis (20). In our study, we showed the changes in chemokine, cytokine and growth factor levels after hUCB-MSCs transfusion in MCT induced PAH rats. Of these factors, immunomodulation and inflammation regulated by various types of cytokines are some of the key pathways which interact with each other in hUCB-MSCs and PAH. Our present study provides an understanding of the biology of hUCB-MSCs therapy and use of anti-cytokine and growth factor therapies.

Recently, in a well-established PAH model, it has been demonstrated that MSC injection can have a favorable effect on pulmonary vasculature, pulmonary pressure and RV structure and function (21). MSC is regarded to have an effect on cardiovascular disease, degenerative joint disease and acute lung injury. And the expected effectiveness of MSC is to increase anti-inflammatory cytokines, positive neurohormonal response and positive pulmonary vascular remodeling (22). MSC can be considered to be acquired from the umbilical cord at present (23). Adult stem cells are helpful in treating and repairing injured tissues and it can be an alternative source of embryonic stem cells. The transplantation of cord blood has been part of clinical practice for more than 10 yr (24). Randomized and nonrandomized clinical trials have been tried with a variety of stem cells, including bone marrow derived cells, endothelial precursor cells and MSC (25). However, it is still a controversial issue whether MSCs from human umbilical cord blood are capable of differentiation into pulmonary vascular epithelial cells in vivo (26, 27). Recent studies confirmed that MSCS, hematopoietic stem cells and other populations could successfully structurally engraft upon mature differentiated airway and alveolar epithelial (28, 29).

Meanwhile, administration of hUCB-MSCs via the external jugular vein route used in this study did not cause an immune response and there was a high probability to arrive at the designated site in the lung. In 2009, there was a report that a direct administration of hUCB-MSCs to neonatal rats by the trachea decreased inflammation related factors in the lung more effectively than intraperitoneal injection. Because they did not use the same dose of hUCB-MSCs, direct comparison between our study is difficult (30). In 2006, in Barber's study, MSCs improved blood vessel endothelial cell functions in MCT induced PAH rat (31). In our present study, endothelial dysfunction was improved.

There are a lot of treatment options for PAH, but an effective therapy still does not exist. Therefore, there may be many possibilities for applications of hUCB-MSCs on PAH. Advantages include decreased pulmonary arteriole thickening and several gene expressions compared with other chemical drugs.

The limitations of our study are as follows. First, the sample

size is small and the follow-up duration is relatively short. Second, we did not check the transdifferentiation of hUCB-MSC and just confirmed hUCB-MSCs engraftment. It is considered that further studies about transdifferentiation are needed.

Future studies with larger sample sizes and a longer follow-up duration will be required to determine the appropriate amount of hUCB-MSCs, frequency and time interval required for PAH treatment.

DISCLOSURE

The authors have no conflicts of interest to disclose.

AUTHOR CONTRIBUTION

Conceived and designed the experiments:Hong YM, Kim KC. Performed the expriments: Lee HR, Lee JC, Kwon JH, Kim KC, Cho MS, Yang YS, O W, Choi SJ, Seo ES, Wang TJ. Drafting of the manuscript: Lee HR. Critical revision of the manuscript for important intellectual content: Hong YM, Lee HR. Statistical analysis: Lee HR, Lee JC. Administrative, technical, or material support: Hong YM, Kim KC.

ORCID

Hyeryon Lee *http://orcid.org/0000-0002-8566-7503*
Jae Chul Lee *http://orcid.org/0000-0002-6539-0922*
Jung Hyun Kwon *http://orcid.org/0000-0002-1388-3696*
Kwan Chang Kim *http://orcid.org/0000-0001-8297-5415*
Min-Sun Cho *http://orcid.org/0000-0001-8772-9686*
Yoon Sun Yang *http://orcid.org/0000-0002-5793-6104*
Wonil Oh *http://orcid.org/0000-0002-6349-738X*
Soo Jin Choi *http://orcid.org/0000-0002-7885-4212*
Eun-Seok Seo *http://orcid.org/0000-0003-3465-3846*
Sang-Joon Lee *http://orcid.org/0000-0003-3286-5941*
Tae Jun Wang *http://orcid.org/0000-0002-2870-7046*
Young Mi Hong *http://orcid.org/0000-0002-6600-7876*

REFERENCES

1. Martin KB, Klinger JR, Rounds SI. *Pulmonary arterial hypertension: new insights and new hope. Respirology 2006; 11: 6-17.*
2. Chamberlain G, Fox J, Ashton B, Middleton J. *Concise review: mesenchymal stem cells: their phenotype, differentiation capacity, immunological features, and potential for homing. Stem Cells 2007; 25: 2739-49.*
3. Budhiraja R, Tuder RM, Hassoun PM. *Endothelial dysfunction in pulmonary hypertension. Circulation 2004; 109: 159-65.*
4. Giaid A, Saleh D. *Reduced expression of endothelial nitric oxide synthase in the lungs of patients with pulmonary hypertension. N Engl J Med 1995; 333: 214-21.*
5. Mason NA, Springall DR, Burke M, Pollock J, Mikhail G, Yacoub MH, Polak JM. *High expression of endothelial nitric oxide synthase in plexiform lesions of pulmonary hypertension. J Pathol 1998; 185: 313-8.*
6. Zhao L, Mason NA, Morrell NW, Kojonazarov B, Sadykov A, Maripov A, Mirrakhimov MM, Aldashev A, Wilkins MR. *Sildenafil inhibits hypoxia-induced pulmonary hypertension. Circulation 2001; 104: 424-8.*
7. Gomez-Arroyo JG, Farkas L, Alhussaini AA, Farkas D, Kraskauskas D, Voelkel NF, Bogaard HJ. *The monocrotaline model of pulmonary hypertension in perspective. Am J Physiol Lung Cell Mol Physiol 2012; 302: L363-9.*
8. Ryan J, Bloch K, Archer SL. *Rodent models of pulmonary hypertension: harmonisation with the world health organisation's categorisation of human PH. Int J Clin Pract Suppl 2011: 15-34.*
9. Beppu H. *Transgenic and knockout mouse models for pulmonary hypertension: role of BMPR2: Part I: Genetically manipulated mouse models of pulmonary vascular disease and lung injury. Drug Discov Today 2010; 7: 61-5.*
10. Lee M, Jeong SY, Ha J, Kim M, Jin HJ, Kwon SJ, Chang JW, Choi SJ, Oh W, Yang YS, et al. *Low immunogenicity of allogeneic human umbilical cord blood-derived mesenchymal stem cells in vitro and in vivo. Biochem Biophys Res Commun 2014; 446: 983-9.*
11. Park JH, Hwang I, Hwang SH, Han H, Ha H. *Human umbilical cord blood-derived mesenchymal stem cells prevent diabetic renal injury through paracrine action. Diabetes Res Clin Pract 2012; 98: 465-73.*
12. Koo HS, Kim KC, Hong YM. *Gene expressions of nitric oxide synthase and matrix metalloproteinase-2 in monocrotaline-induced pulmonary hypertension in rats after bosentan treatment. Korean Circ J 2011; 41: 83-90.*
13. Kim KC, Lee HR, Kim SJ, Cho MS, Hong YM. *Changes of gene expression after bone marrow cell transfusion in rats with monocrotaline-induced pulmonary hypertension. J Korean Med Sci 2012; 27: 605-13.*
14. Yang SE, Ha CW, Jung M, Jin HJ, Lee M, Song H, Choi S, Oh W, Yang YS. *Mesenchymal stem/progenitor cells developed in cultures from UC blood. Cytotherapy 2004; 6: 476-86.*
15. O'Callaghan DS, Savale L, Yaïci A, Natali D, Jaïs X, Parent F, Montani D, Humbert M, Simonneau G, Sitbon O. *Endothelin receptor antagonists for the treatment of pulmonary arterial hypertension. Expert Opin Pharmacother 2011; 12: 1585-96.*
16. Zhang H, Fazel S, Tian H, Mickle DA, Weisel RD, Fujii T, Li RK. *Increasing donor age adversely impacts beneficial effects of bone marrow but not smooth muscle myocardial cell therapy. Am J Physiol Heart Circ Physiol 2005; 289: H2089-96.*
17. Rocha V, Cornish J, Sievers EL, Filipovich A, Locatelli F, Peters C, Remberger M, Michel G, Arcese W, Dallorso S, et al. *Comparison of outcomes of unrelated bone marrow and umbilical cord blood transplants in children with acute leukemia. Blood 2001; 97: 2962-71.*
18. Dranoff G. *Cytokines in cancer pathogenesis and cancer therapy. Nat Rev Cancer 2004; 4: 11-22.*
19. Munoz RM, Han H, Tegeler T, Petritis K, Von Hoff DD, Hoffman SA. *Isolation and characterization of muscle fatigue substance with anti-tumor activities. J Cancer 2013; 4: 343-9.*
20. Duncan M, Wagner BD, Murray K, Allen J, Colvin K, Accurso FJ, Ivy DD. *Circulating cytokines and growth factors in pediatric pulmonary hypertension. Mediators Inflamm 2012; 2012: 143428.*
21. Sahara M, Sata M, Morita T, Nakamura K, Hirata Y, Nagai R. *Diverse contribution of bone marrow-derived cells to vascular remodeling associat-*

 http://dx.doi.org/10.3346/jkms.2015.30.5.576

ed with pulmonary arterial hypertension and arterial neointimal formation. Circulation 2007; 115: 509-17.

22. Angelini A, Castellani C, Ravara B, Franzin C, Pozzobon M, Tavano R, Libera LD, Papini E, Vettor R, De Coppi P, et al. *Stem-cell therapy in an experimental model of pulmonary hypertension and right heart failure: role of paracrine and neurohormonal milieu in the remodeling process. J Heart Lung Transplant 2011; 30: 1281-93.*
23. Erices A, Conget P, Minguell JJ. *Mesenchymal progenitor cells in human umbilical cord blood. Br J Haematol 2000; 109: 235-42.*
24. Boudoulas KD, Hatzopoulos AK. *Cardiac repair and regeneration: the Rubik's cube of cell therapy for heart disease. Dis Model Mech 2009; 2: 344-58.*
25. Sueblinvong V, Loi R, Eisenhauer PL, Bernstein IM, Suratt BT, Spees JL, Weiss DJ. *Derivation of lung epithelium from human cord blood-derived mesenchymal stem cells. Am J Respir Crit Care Med 2008; 177: 701-11.*
26. Wu KH, Zhou B, Lu SH, Feng B, Yang SG, Du WT, Gu DS, Han ZC, Liu YL. *In vitro and in vivo differentiation of human umbilical cord derived stem cells into endothelial cells. J Cell Biochem 2007; 100: 608-16.*
27. Fan CG, Zhang QJ, Zhou JR. *Therapeutic potentials of mesenchymal stem cells derived from human umbilical cord. Stem Cell Rev 2011; 7: 195-207.*
28. Loi R, Beckett T, Goncz KK, Suratt BT, Weiss DJ. *Limited restoration of cystic fibrosis lung epithelium in vivo with adult bone marrow-derived cells. Am J Respir Crit Care Med 2006; 173: 171-9.*
29. Nauta AJ, Fibbe WE. *Immunomodulatory properties of mesenchymal stromal cells. Blood 2007; 110: 3499-506.*
30. Chang YS, Oh W, Choi SJ, Sung DK, Kim SY, Choi EY, Kang S, Jin HJ, Yang YS, Park WS. *Human umbilical cord blood-derived mesenchymal stem cells attenuate hyperoxia-induced lung injury in neonatal rats. Cell Transplant 2009; 18: 869-86.*
31. Baber SR, Deng W, Master RG, Bunnell BA, Taylor BK, Murthy SN, Hyman AL, Kadowitz PJ. *Intratracheal mesenchymal stem cell administration attenuates monocrotaline-induced pulmonary hypertension and endothelial dysfunction. Am J Physiol Heart Circ Physiol 2007; 292: H1120-8.*